

**Mode selectivity of dynamically induced conformation in many-body chainlike bead-spring models**Yoshiyuki Y. Yamaguchi <sup>\*</sup>*Graduate School of Informatics, Kyoto University, Kyoto 606-8501, Japan*

(Received 6 September 2022; revised 6 March 2023; accepted 1 June 2023; published 26 June 2023)

We consider conformation of a chain consisting of beads connected by stiff springs, where the conformation is determined by the bending angles between the consecutive two springs. Stability of a conformation is determined intrinsically by a potential energy function depending on the bending angles. However, effective forces induced by excited springs can change the stability, and a conformation can stay around a local maximum or a saddle of the bending potential. A stabilized conformation was named the dynamically induced conformation in a previous work on a three-body system [Y. Y. Yamaguchi *et al.*, *Phys. Rev. E* **105**, 064201 (2022)]. A remarkable fact is that the stabilization by the spring motion depends on the excited normal modes, which depend on a conformation. We extend analyses of the dynamically induced conformation in many-body chainlike bead-spring systems. Simple rules are that the lowest-eigenfrequency mode contributes to the stabilization and that the higher the eigenfrequency is, the more the destabilization emerges. We verify theoretical predictions by performing numerical simulations.

DOI: [10.1103/PhysRevE.107.064212](https://doi.org/10.1103/PhysRevE.107.064212)**I. INTRODUCTION**

Conformation has a deep relationship to function as found in isomerization. Maintenance of a conformation requires stability, and the stability is usually associated with the landscape of a given potential energy function. We however underline that the dynamics also contributes to the stability of conformation.

A typical example of the dynamical stabilization is the Kapitza pendulum [1–4], which is an inverted pendulum under uniform gravity. The inverted pendulum is intrinsically unstable, but it is stabilized by an effective force induced by fast vertical oscillation of the pivot. The existence of two timescales, the slow pendulum and the fast pivot, is the key mechanism of this stabilization. Owing to the importance of the mechanism, this highly nonintuitive stabilization is applied in a wide variety of fields: many-body coupled pendulums [5], microscopic objects with a surrounding medium [6], particles on a toroidal helix [7], liquid [8,9], control [10,11], localized wave packets in a repulsive Bose-Einstein condensate [12], optical molasses [13], quantum versions [14–17], and complex potential versions [18].

In this article a similar dynamical stabilization of conformation is presented in a bead-spring model [19], which is a model of polymers. The model consists of the beads connected by stiff springs and is an autonomous Hamiltonian system. We explain the meaning of stabilization in an autonomous system, since there is no external force modifying the system. It is important to divide the system into two parts: the slow conformation part defined by the angles of nearby springs and the fast spring part. We focus on the subsystem of the conformation part, for which the spring

part plays the role of the rapidly oscillating external force of the Kapitza pendulum. Let us start from the zero spring energy. In that case, stability of a conformation is ruled by the given bending potential energy function: A conformation is stable if it is at a local minimum of the bending potential and unstable at a saddle or a local maximum. However, the bending part is not independent of the spring part. Excitation of the fast spring part induces additional effective forces on the conformation part, and the effective forces can modify the stability ruled by the bending potential. For instance, a local maximum of the bending potential can become a local minimum of the effective potential, as the spring energy increases [20]. The meaning of the dynamical stabilization is therefore the stabilization of a nonlocal-minimum point of the bending potential by exciting the spring part. A dynamically stabilized conformation is called a dynamically induced conformation (DIC) [20].

The dynamical stabilization in the bead-spring model was first observed in numerical simulations without the bending potential [21] and then analyzed theoretically in the three-body model having a bending potential [20] with the aids of the multiple-scale analysis [22] and the averaging method [23–25]. A surprising result of the theory is that the stability of a conformation depends on the excited normal modes of the springs. Suppose that the system consists of three equal masses and two identical springs. The in-phase mode contributes to stabilize (destabilize) the straight (fully bent) conformation and the antiphase mode to destabilize (stabilize) the straight (fully bent) conformation. Here the in-phase (the antiphase) mode is a normal mode of the springs and is defined as the two springs expanding and contracting simultaneously (alternatively).

The mode dependence of stabilization provides a sharp contrast with the Kapitza pendulum, since the oscillating external force always contributes to stabilize the inverted

<sup>\*</sup>yyama@amp.i.kyoto-u.ac.jp

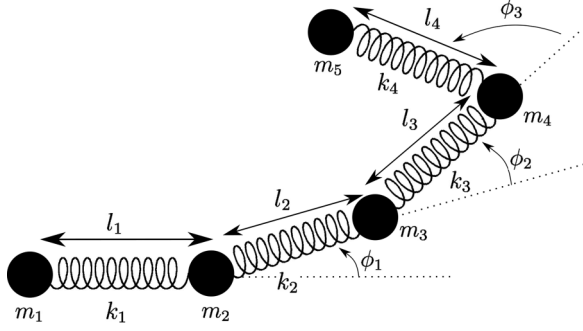


FIG. 1. Chainlike bead-spring model for  $\mathbb{R}^2$ . This diagram shows an example of  $N = 5$  (five beads connected by four springs).

pendulum irrespective of the phase of the external force. This aspect motivates us to extend the previous analysis [20], which is restricted to three-body systems. The aim of this article is to answer the following questions in chainlike bead-spring models through the combination of the theory and numerical simulations: Is DIC ubiquitous? How does the stabilization of a conformation depend on the excited normal modes? Is there a simple rule for the dependence?

The dynamical effective force is not specific in the bead-spring model. A related dynamical effect has been discussed in the reaction dynamics of atomic clusters [26–29]. The present study then is also important in the context of conformational isomerization in flexible molecules. It is experimentally observed in *N*-acetyl-tryptophan methyl amide that the population of isomers is modified by exciting vibration in a bond, and the modified population depends on the excited bond [30], whereas the Rice-Ramsperger-Kassel-Marcus theory [31–33] states that the destination is determined statistically. This mode selectivity may have a deep connection to the mode dependence of DIC.

This paper is organized as follows. The chainlike bead-spring model is introduced in Sec. II. We extract the equations of motion for the slow bending motion in Sec. III. Assuming the absence of the bending potential to observe the simplest case, we exhibit theoretically the excited mode dependence of stability in Sec. IV, concentrating on one-dimensional conformations, whose bending angles are 0 or  $\pi$ . The theoretical predictions are examined through numerical simulations in Sec. V by applying the Lennard-Jones potential as the bending potential. Section VI is devoted to a summary and discussion.

## II. MODEL

We consider the  $N$ -body chainlike bead-spring model for  $\mathbb{R}^2$ . No gravitational force is applied. The model consists of  $N$  beads connected by  $N - 1$  springs. The  $i$ th bead is characterized by the mass  $m_i \in (0, \infty)$ , the position column vector  $\mathbf{r}_i \in \mathbb{R}^2$ , and the velocity column vector  $\dot{\mathbf{r}}_i = d\mathbf{r}_i/dt \in \mathbb{R}^2$ , where  $t \in \mathbb{R}$  is the time. (See Fig. 1 for a schematic diagram of the system.) We will input a bending potential energy in addition to the spring potential energy.

The system has translational symmetry, which induces conservation of the total momentum vector. We set it as the zero vector and neglect it. This reduction is realized by

introducing the internal coordinates

$$\begin{aligned} \mathbf{y} &= \begin{pmatrix} \mathbf{l} \\ \boldsymbol{\phi} \end{pmatrix} \in \mathbb{R}^{2N-2}, \\ \mathbf{l} &= (l_1, \dots, l_{N-1})^T \in \mathbb{R}^{N-1}, \\ \boldsymbol{\phi} &= (\phi_1, \dots, \phi_{N-1})^T \in \mathbb{R}^{N-1}, \end{aligned} \quad (1)$$

where the superscript T represents transposition. The vector  $\mathbf{l}$  contains the lengths of the springs

$$l_i = \|\mathbf{r}_{i+1} - \mathbf{r}_i\|, \quad i = 1, \dots, N - 1 \quad (2)$$

and the natural lengths of the springs are defined as  $\mathbf{l}_* = (l_{1,*}, \dots, l_{N-1,*})^T$ . The vector  $\boldsymbol{\phi}$  contains the bending angles between the adjacent springs, which satisfy

$$\cos \phi_i = \frac{(\mathbf{r}_{i+2} - \mathbf{r}_{i+1}) \cdot (\mathbf{r}_{i+1} - \mathbf{r}_i)}{\|\mathbf{r}_{i+2} - \mathbf{r}_{i+1}\| \|\mathbf{r}_{i+1} - \mathbf{r}_i\|}, \quad i = 1, \dots, N - 2, \quad (3)$$

where the centered dot represents the Euclidean inner product and  $\|\dots\|$  the Euclidean norm. The last angle  $\phi_{N-1}$  is associated with the rotational symmetry of the system and is a cyclic coordinate. We keep it to simplify computations. As we will see, the internal coordinates are useful to clarify coupling between the springs  $\mathbf{l}$  and the bending angles  $\boldsymbol{\phi}$ .

The Lagrangian of the model is written as

$$L(\mathbf{y}, \dot{\mathbf{y}}) = \frac{1}{2} \sum_{\alpha, \beta=1}^{2N-2} B^{\alpha\beta}(\mathbf{y}) \dot{y}_\alpha \dot{y}_\beta - V(\mathbf{y}), \quad (4)$$

where  $V(\mathbf{y})$  is the total potential energy function. The function  $B^{\alpha\beta}(\mathbf{y})$  is the  $(\alpha, \beta)$  element of the matrix  $\mathbf{B}(\mathbf{y}) \in \text{Mat}(2N - 2)$ . Here  $\text{Mat}(n)$  represents the set of real square matrices of size  $n$ . We will use the above notation for any matrices. The explicit form of  $\mathbf{B}(\mathbf{y})$  is given in Appendix A 1. Note that, in general, an arabic alphabetic index runs from 1 to  $N - 1$  and a greek alphabetic index runs from 1 to  $2N - 2$ .

From now on, we adopt the Einstein notation for the sum: We take the sum over an index if it appears twice in a term. The Euler-Lagrange equation for the variable  $y_\alpha$  ( $\alpha = 1, \dots, 2N - 2$ ) is expressed as

$$B^{\alpha\beta}(\mathbf{y}) \ddot{y}_\beta + \left( \frac{\partial B^{\alpha\beta}}{\partial y_\gamma}(\mathbf{y}) - \frac{1}{2} \frac{\partial B^{\beta\gamma}}{\partial y_\alpha}(\mathbf{y}) \right) \dot{y}_\beta \dot{y}_\gamma + \frac{\partial V}{\partial y_\alpha}(\mathbf{y}) = 0. \quad (5)$$

## III. THEORY

This section provides a general theory to derive the equations of motion which describe the slow bending motion affected by the fast spring motion. We analyze the Euler-Lagrange equations (5) perturbatively by introducing a small parameter  $\epsilon$ , which represents separation of the two timescales between the fast spring motion and the slow bending motion.

### A. Expansions of variables

We assume that there exist two timescales:  $t_0 = t$  corresponds to the fast spring motion and  $t_1 = \epsilon t$  ( $0 < \epsilon \ll 1$ ) to the slow bending motion. The two timescales induce the

expansion

$$\frac{d}{dt} = \frac{\partial}{\partial t_0} + \epsilon \frac{\partial}{\partial t_1}. \quad (6)$$

We also assume that the expansions

$$\begin{aligned} \mathbf{l}(t_0, t_1) &= \mathbf{l}_* + \epsilon \mathbf{l}^{(1)}(t_0, t_1), \\ \boldsymbol{\phi}(t_0, t_1) &= \boldsymbol{\phi}^{(0)}(t_1) + \epsilon \boldsymbol{\phi}^{(1)}(t_0, t_1) \end{aligned} \quad (7)$$

are valid, which are summarized as

$$\mathbf{y}(t_0, t_1) = \mathbf{y}^{(0)}(t_1) + \epsilon \mathbf{y}^{(1)}(t_0, t_1). \quad (8)$$

Hereafter the superscript with the parentheses represents the order of  $\epsilon$ . We are interested in the large and slow motion of the bending angles  $\boldsymbol{\phi}^{(0)}(t_1)$  and its stability.

The velocities  $\dot{\mathbf{l}}_i$  and  $\dot{\boldsymbol{\phi}}_i$  are of the same order  $O(\epsilon)$  and the fastness of motion connotes a short period. Indeed, the period of a normal mode is of  $O(\epsilon^0)$ , while the period of the large bending motion is of  $O(\epsilon^{-1})$ .

We note that the assumptions (6) and (8) lead to the decomposition of potential up to  $O(\epsilon^2)$  as

$$V(\mathbf{y}) = V_{\text{spring}}(\mathbf{l}) + U_{\text{bend}}(\mathbf{y}) \quad (9)$$

and

$$U_{\text{bend}}(\mathbf{y}) = \epsilon^2 U_{\text{bend}}^{(2)}(\boldsymbol{\phi}^{(0)}) + O(\epsilon^3), \quad (10)$$

where  $V_{\text{spring}}$  and  $U_{\text{bend}}$  are the spring energy and the bending energy, respectively. (See Appendix B for details.) We can set  $V_{\text{spring}}(\mathbf{l}_*) = 0$  without loss of generality, and the total energy  $E$  is expanded as

$$E = \epsilon^2 E^{(2)} + O(\epsilon^3). \quad (11)$$

### B. Origin of the dependence on the excited normal modes and total energy

Substituting Eqs. (6) and (8) into Eq. (5), we have the expanded equations of motion for each order of  $\epsilon$ . We sketch the theory to highlight the excited mode dependence of stabilization.

The leading terms are of  $O(\epsilon)$ , which give the linear equations

$$\frac{\partial^2 \mathbf{y}^{(1)}}{\partial t_0^2} = -\mathbf{X}(\mathbf{y}^{(0)}(t_1)) \mathbf{y}^{(1)}, \quad (12)$$

where

$$\mathbf{X}(\mathbf{y}) = [\mathbf{B}(\mathbf{y})]^{-1} \mathbf{K} \in \text{Mat}(2N - 2), \quad (13)$$

with

$$\mathbf{K} = \begin{pmatrix} \mathbf{K}_l & \mathbf{O} \\ \mathbf{O} & \mathbf{O} \end{pmatrix} \in \text{Mat}(2N - 2). \quad (14)$$

The matrix  $\mathbf{K}_l$  is the Hessian of  $V_{\text{spring}}(\mathbf{l})$  at  $\mathbf{l}_*$ :

$$(K_l)^{ij} = \frac{\partial^2 V_{\text{spring}}}{\partial l_i \partial l_j}(\mathbf{l}_*), \quad i, j = 1, \dots, N - 1. \quad (15)$$

We assume that  $\mathbf{K}_l$  is positive definite. There exist  $N - 1$  oscillating normal modes and we denote their amplitudes and phases by  $\mathbf{w} = (w_1, \dots, w_{N-1})$  and  $\boldsymbol{\delta} = (\delta_1, \dots, \delta_{N-1})$ , respectively.

The slow bending motion  $\boldsymbol{\phi}^{(0)}(t_1)$  is captured in  $O(\epsilon^2)$ , where the fast oscillations of  $\mathbf{y}^{(1)}(t_0, t_1)$  are included. We eliminate the fast timescale  $t_0$  by performing the averaging over  $t_0$ . This averaging also eliminates the  $N - 1$  phases  $\boldsymbol{\delta}$ , but the  $N - 1$  amplitudes  $\mathbf{w}$  remain and may depend on the slow timescale  $t_1$ . We then introduce a working hypothesis [20]

$$w_i(t_1)^2 = v_i w(t_1)^2, \quad i = 1, \dots, N - 1, \quad (16)$$

which is inspired by the adiabatic invariance. The prefactors  $v_i$  represent the initial distribution of energy among the  $N - 1$  normal modes and are assumed to be constant in time. The hypothesis can be rewritten as

$$E_i^{(2)} = v_i E_{\text{normal}}^{(2)}, \quad i = 1, \dots, N - 1 \quad (17)$$

where  $E_{\text{normal}}^{(2)}$  is the second-order normal mode energy and  $E_i^{(2)}$  is the contribution from the  $i$ th normal mode. Due to the hypothesis (16), the number of unknown time series is reduced from  $N - 1$  to one, i.e.,  $w(t_1)$ , and we eliminate the last one by using the energy conservation law. Finally, we obtain the closed equations of motion for  $\boldsymbol{\phi}^{(1)}(t_1)$ , and the equations depend on the ratios of the excited normal modes

$$\mathbf{N} = \begin{pmatrix} \mathbf{N}_l & \mathbf{O} \\ \mathbf{O} & \mathbf{O} \end{pmatrix}, \quad \mathbf{N}_l = \text{diag}(v_1, \dots, v_{N-1}) \quad (18)$$

and energy  $E^{(2)}$ .

### C. Equations of motion for the slow bending motion

Following the theory sketched in Sec. III B, we obtain the closed equations of motion for the slow bending variables  $\boldsymbol{\phi}^{(0)}(t_1)$  as

$$\frac{d^2 \phi_i^{(0)}}{dt_1^2} + F_i^{jn}(\mathbf{y}^{(0)}) \frac{d\phi_j^{(0)}}{dt_1} \frac{d\phi_n^{(0)}}{dt_1} + G_i(\mathbf{y}^{(0)}) = 0 \quad (19)$$

for  $i = 1, \dots, N - 1$ . (See Appendix A 2 for details.) The functions  $F_i^{jn}$  and  $G_i$  are

$$F_i^{jn}(\mathbf{y}) = [B_{\phi\phi}^{-1}]^{is} \left( \frac{\partial B_{\phi\phi}^{sj}}{\partial \phi_n} - \frac{1}{2} \frac{\partial B_{\phi\phi}^{jn}}{\partial \phi_s} + \frac{1}{4} \mathcal{T}_s B_{\phi\phi}^{jn} \right) \quad (20)$$

and

$$G_i(\mathbf{y}) = [B_{\phi\phi}^{-1}]^{is} \left( \frac{\partial U_{\text{bend}}^{(2)}}{\partial \phi_s} - \frac{E^{(2)} - U_{\text{bend}}^{(2)}}{2} \mathcal{T}_s \right), \quad (21)$$

where  $s = 1, \dots, N - 1$ . We underline that the  $(2N - 2)$ -dimensional full dynamics (5) is reduced to the  $(N - 1)$ -dimensional dynamics (19), which describes the subsystem of the slow bending motion. Explanations of the symbols follow.

The functions  $\mathcal{T}_s$  represent the dynamical effects coming from the averaging procedure of the fast normal modes. If  $\mathcal{T}_s \equiv 0$  ( $s = 1, \dots, N - 1$ ), Eq. (19) represents motion of  $\boldsymbol{\phi}^{(0)}$  governed solely by the bending potential  $U_{\text{bend}}^{(2)}(\boldsymbol{\phi}^{(0)})$ . Their explicit forms are

$$\mathcal{T}_s(\mathbf{y}) = \begin{cases} \text{Tr}(\mathbf{P}^T \frac{\partial \mathbf{B}}{\partial \phi_s} \mathbf{P} \mathbf{A} \mathbf{N}) / \text{Tr}(\mathbf{P}^T \mathbf{K} \mathbf{P} \mathbf{N}), & \mathbf{N} \neq \mathbf{O} \\ 0, & \mathbf{N} = \mathbf{O}. \end{cases} \quad (22)$$

The matrix  $\mathbf{P} \in \text{Mat}(2N - 2)$  diagonalizes the matrix  $\mathbf{X}$  as  $\mathbf{XP} = \mathbf{P}\mathbf{\Lambda}$  and the diagonal matrix  $\mathbf{\Lambda}$  contains the eigenvalues of  $\mathbf{X}$  as

$$\mathbf{\Lambda} = \begin{pmatrix} \mathbf{\Lambda}_l & \mathbf{O} \\ \mathbf{O} & \mathbf{O} \end{pmatrix}, \quad \mathbf{\Lambda}_l = \text{diag}(\lambda_1, \dots, \lambda_{N-1}), \quad (23)$$

where  $\lambda_1 \leq \dots \leq \lambda_{N-1}$  are the nontrivial eigenvalues.

We decomposed the matrix  $\mathbf{B} \in \text{Mat}(2N - 2)$  into four square submatrices of size  $N - 1$  as

$$\mathbf{B}(\mathbf{y}) = \begin{pmatrix} \mathbf{B}_{ll}(\boldsymbol{\phi}) & \mathbf{B}_{l\phi}(\mathbf{y}) \\ \mathbf{B}_{\phi l}(\mathbf{y}) & \mathbf{B}_{\phi\phi}(\mathbf{y}) \end{pmatrix}. \quad (24)$$

See Eq. (A10) for explicit forms of the submatrices.

We use the same symbol  $E^{(2)}$  for the averaged  $E^{(2)}$  over the fast timescale  $t_0$  for simplicity of notation. It is read with the hypothesis (16) as

$$E^{(2)} = \frac{1}{2} \text{Tr} \left[ \mathbf{B}_{\phi\phi}(\mathbf{y}^{(0)}) \frac{d\boldsymbol{\phi}^{(0)}}{dt_1} \left( \frac{d\boldsymbol{\phi}^{(0)}}{dt_1} \right)^T \right] + U_{\text{bend}}^{(2)}(\boldsymbol{\phi}^{(0)}) + \frac{w(t_1)^2}{2} \text{Tr}(\mathbf{P}^T \mathbf{K} \mathbf{P} \mathbf{N}). \quad (25)$$

The last term of Eq. (25) is the averaged normal mode energy  $\langle E_{\text{normal}}^{(2)} \rangle$ . We used Eq. (25) to eliminate the last unknown variable  $w(t_1)^2$  and to derive Eq. (19).

#### D. Remarks

We make four remarks regarding Eq. (19). They concern the applicability and restriction of the theory.

First, the spring potential  $V_{\text{spring}}$  is included in Eq. (19) only as the Hessian matrix  $\mathbf{K}_l$ . Thus the linear parts of the springs are essential in the present theory.

Second, the size of the matrices appearing in  $\mathcal{T}_s$  [Eq. (22)] and  $E^{(2)}$  [Eq. (25)] can be reduced from  $2N - 2$  to  $N - 1$ . (See Appendix C for details.)

Third, the numbering of normal modes is important for the hypothesis (16), but a global numbering is not trivial in general because eigenvalues of  $\mathbf{X}(\mathbf{y}^{(0)})$  may cross by varying  $\boldsymbol{\phi}^{(0)}$  as shown in Fig. 2. Nevertheless, the numbers can be identified in a local region of  $\boldsymbol{\phi}^{(0)}$ , and it is sufficient to study the stationarity and stability of a conformation. From now on, we number the modes locally in ascending order of the eigenvalues unless otherwise stated.

Fourth, it is not easy to construct a global effective potential representing Eq. (19), while the three-body system has it [20]. Moreover, it is not clear whether Eq. (19) is a potential system.

#### IV. DYNAMICAL STABILITY

In this section we study the stability of stationary conformations in the absence of the bending potential  $U_{\text{bend}} \equiv 0$  to shed light on the dynamical contribution. No bending potential implies that any stationary conformation is marginal if no normal modes are excited. However, it may be stable or unstable in Eq. (19) due to the dynamically added terms  $\mathcal{T}_s$ .

In a chainlike system, the matrix  $\mathbf{K}_l$  is diagonal as

$$\mathbf{K}_l = \text{diag}(k_1, \dots, k_{N-1}). \quad (26)$$

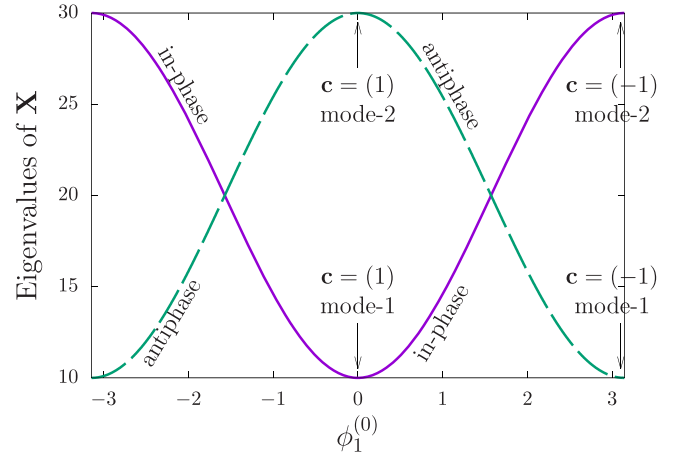


FIG. 2. Two eigenvalues of  $\mathbf{X}$ , which depend on  $\phi_1^{(0)}$  for  $N = 3$ , for the in-phase mode (purple solid line) and the antiphase mode (green dashed line), with  $m_1 = m_2 = m_3 = m = 1$  and  $\mathbf{K}_l = \text{diag}(k, k)$  for  $k = 10$ . The eigenvalues are  $(k/m)(2 \mp \cos \phi_1^{(0)})$ . The modes are locally numbered in ascending order of the eigenvalues. The conformation symbol  $\mathbf{c}$  is defined in Sec. IV B:  $\mathbf{c} = (1)$  represents the straight conformation and  $\mathbf{c} = (-1)$  the fully bent conformation.

Further, we restrict ourselves to the uniform setting

$$m_i = m, \quad k_j = k, \quad l_{j,*} = l_*, \quad 1 \leq i \leq N, \quad 1 \leq j \leq N - 1 \quad (27)$$

and to the one-dimensional conformations defined in Sec. IV B. From now on, we replace  $G_i(\mathbf{y}^{(0)})$  with  $G_i(\boldsymbol{\phi}^{(0)})$ , for instance, to highlight the dependence on the variables, since  $\mathbf{y}^{(0)} = (\mathbf{l}_*, \boldsymbol{\phi}^{(0)})$  and  $\mathbf{l}_*$  is a constant vector.

#### A. Stationary point and stability

Equation (19) is rewritten as

$$\frac{d\phi_i^{(0)}}{dt_1} = v_i, \quad \frac{dv_i}{dt_1} = -F_i^{jn}(\boldsymbol{\phi}^{(0)})v_j v_n - G_i(\boldsymbol{\phi}^{(0)}), \quad (28)$$

where  $\mathbf{v} = (v_1, \dots, v_{N-1})^T$  and  $v_i = d\phi_i^{(0)}/dt_1$ . The stationary condition is

$$\boldsymbol{\Phi}_{\text{st}} = \begin{pmatrix} \boldsymbol{\phi}_{\text{st}}^{(0)} \\ \mathbf{v}_{\text{st}} \end{pmatrix} : \text{stationary} \iff \begin{cases} \mathbf{G}(\boldsymbol{\phi}_{\text{st}}^{(0)}) = \mathbf{0} \\ \mathbf{v}_{\text{st}} = \mathbf{0}, \end{cases} \quad (29)$$

where  $\mathbf{G} = (G_1, \dots, G_{N-1})^T$ . The stability of a stationary state  $\boldsymbol{\Phi}_{\text{st}}$  is determined by the Jacobian matrix

$$\mathbf{J}(\boldsymbol{\Phi}_{\text{st}}) = \begin{pmatrix} \mathbf{O} & \mathbf{E} \\ -D_{\boldsymbol{\phi}} \mathbf{G}(\boldsymbol{\phi}_{\text{st}}^{(0)}) & \mathbf{O} \end{pmatrix} \in \text{Mat}(2N - 2). \quad (30)$$

Here  $D_{\boldsymbol{\phi}} \mathbf{G}$  is the Jacobian matrix of  $\mathbf{G}$  with respect to the variables  $\boldsymbol{\phi}^{(0)}$ .

Our task is to compute the eigenvalues of  $D_{\boldsymbol{\phi}} \mathbf{G}$  because the eigenvalues of  $\mathbf{J}$  are obtained from the eigenvalues of  $D_{\boldsymbol{\phi}} \mathbf{G}$ . Let us assume that the matrix  $D_{\boldsymbol{\phi}} \mathbf{G}(\boldsymbol{\phi}_{\text{st}}^{(0)})$  is diagonalizable and has the eigenvalues  $g_1, \dots, g_{N-1}$ . Then the eigenvalues of  $\mathbf{J}(\boldsymbol{\Phi}_{\text{st}})$  are  $\pm\sqrt{-g_1}, \dots, \pm\sqrt{-g_{N-1}}$ . From this fact, we call an eigenvalue  $g_i$  a stable eigenvalue if  $g_i \in (0, \infty)$ ,

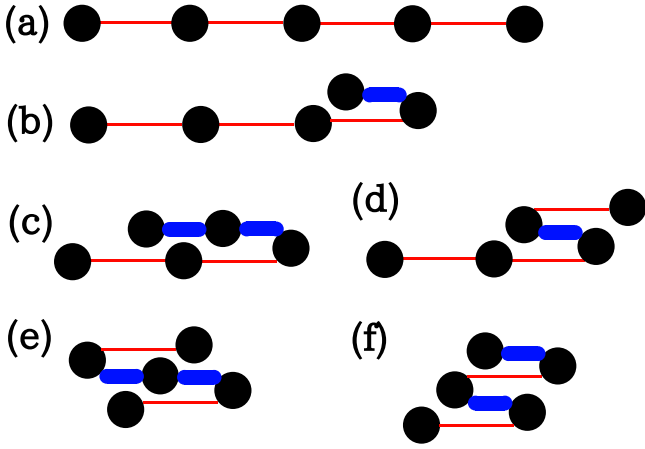


FIG. 3. Illustration of the one-dimensional conformations for  $N = 5$ . The stabilizing mode is characterized by the two types of bonds: A red thin (blue thick) bond represents that the spring is initially longer (shorter) than the natural length. Conformation symbols are (a)  $\mathbf{c} = (1, 1, 1)$ , (b)  $\mathbf{c} = (1, 1, -1)$ , (c)  $\mathbf{c} = (1, -1, 1)$ , (d)  $\mathbf{c} = (1, -1, -1)$ , (e)  $\mathbf{c} = (-1, 1, -1)$ , and (f)  $\mathbf{c} = (-1, -1, -1)$ .

a zero eigenvalue if  $g_i = 0$ , and an unstable eigenvalue if  $g_i \notin [0, \infty)$ .

Two remarks are in order. First, one eigenvalue, denoted by  $g_{N-1}$ , should be zero from the rotational symmetry, and we remove it from the stability criterion. Second, for  $U_{\text{bend}} \equiv 0$ ,  $G_i$  is simplified to

$$G_i(\boldsymbol{\phi}^{(0)}) = -\frac{E^{(2)}}{2} [B_{\phi\phi}^{-1}]^{is} \mathcal{T}_s. \quad (31)$$

Energy  $E^{(2)}$  is a positive overall factor of  $G_i$  and the stability does not depend on  $E^{(2)}$ , while the dependence on  $\mathbf{N}$  remains in  $\mathcal{T}_s$ .

### B. One-dimensional conformations

We focus on the one-dimensional conformations whose set is defined as

$$\mathcal{C}^1 = \{(\phi_1, \dots, \phi_{N-2}) \mid \phi_i \in \{0, \pi\} \ (i = 1, \dots, N-2)\}. \quad (32)$$

In words, the  $i$ th joint of a one-dimensional conformation is straight ( $\phi_i = 0$ ) or fully bent ( $\phi_i = \pi$ ). A conformation in  $\mathcal{C}^1$  is stationary, as proven in Appendix D. The appearance of the bending potential  $U_{\text{bend}}$  forbids  $\phi_i = \pi$  in general, to avoid collision between beads, but we accept  $\phi_i = \pi$  in this section to discuss the simplest case. Later we will perform numerical simulations in the presence of a bending potential which forbids  $\phi_i = \pi$ .

A conformation in  $\mathcal{C}^1$  is symbolized by a sequence of 1 and  $-1$ : The symbol 1 represents the straight joint ( $\phi = 0$ ) and  $-1$  the fully bent joint ( $\phi = \pi$ ). The conformation symbol is denoted by  $\mathbf{c} = (c_1, \dots, c_{N-2})$ . We identify two symmetric conformations like  $(1, -1, -1)$  and  $(-1, -1, 1)$ , because each is mapped to the other by changing the starting end of the chain. All the possible one-dimensional conformations for  $N = 5$  are illustrated in Fig. 3 with their conformation symbols.

### C. Dynamical stability of one-dimensional conformations

We first excite only one normal mode: All the diagonal elements of  $\mathbf{N}$  are zero except for one element. The stability of the one-dimensional conformations is summarized in Table I with dependence on the excited normal mode, where the normal modes are numbered in ascending order of the eigenfrequencies around the conformation considered. Stability is symbolized by S, Z, and U and the number after S, Z, and U represents the number of stable, zero, and unstable nontrivial eigenvalues of  $D_\phi \mathbf{G}$ , respectively, whose sum is  $N - 2$ . A symbol is omitted if the number of corresponding eigenvalues is zero. For instance, the symbol S2U1 represents that the conformation has two stable eigenvalues and one unstable eigenvalue and the conformation is unstable.

The  $(2N - 2)$ -dimensional eigenvector of a normal mode contains the  $(N - 1)$ -dimensional vector corresponding to initial lengths of the springs; the latter vector is characterized by a sequence of  $+$ ,  $0$ , and  $-$ . The symbols  $+$ ,  $0$ , and  $-$  represent that the corresponding spring is initially longer than, equal to, or shorter than the natural length, respectively. For  $N = 3$ , the eigenvector  $(+, +)$  represents the in-phase mode and  $(+, -)$  the antiphase mode. We define the eigenmode symbol as  $\mathbf{s} = (s_1, \dots, s_{N-1})$ .

We have two observations about Table I. First, each conformation is stabilized by the lowest-eigenfrequency mode of the springs. The number of unstable directions increases as the eigenfrequency gets larger. Second, the conformation of two adjacent springs, which is characterized by the angle  $\phi_i$ , is stabilized by simultaneous (alternative) oscillation of the springs when the bending angle is  $\phi_i = 0$  ( $\phi_i = \pi$ ). This stabilization rule is a straightforward extension of the three-body system [20].

Stability analysis can be extended to mixed modes. Analyses for  $N = 3, 4$ , and  $5$  suggest that the dynamical stabilization is ubiquitous in a larger system having multimode excitation. Indeed, the dynamical stabilization is realized with an approximate probability of 0.8 up to  $N = 5$ , whereas higher-eigenfrequency modes contribute to destabilization. (See Appendix E.)

### V. NUMERICAL TESTS

We demonstrate DIC with three examinations of the theory: (i) the threshold of stability, (ii) the validity of the hypothesis (16), and (iii) the robustness of DIC. We assume the uniform setting (27) with

$$m = 1, \quad k = 10, \quad l_* = 1. \quad (33)$$

Throughout this section the small parameter  $\epsilon$  is fixed as  $\epsilon = 10^{-2}$ , the number of beads as  $N = 5$ , and the time step of a fourth-order symplectic integrator [34] as  $\Delta t = 10^{-3}$ . We use the Hamiltonian in Cartesian coordinates

$$H(\mathbf{r}, \mathbf{p}) = \frac{1}{2m} \sum_{i=1}^N \|\mathbf{p}_i\|^2 + V_{\text{spring}}(\mathbf{r}) + U_{\text{bend}}(\mathbf{r}) \quad (34)$$

to make the integrator explicit. Here  $\mathbf{r} = (\mathbf{r}_1, \dots, \mathbf{r}_N)$  are the positions and  $\mathbf{p} = (\mathbf{p}_1, \dots, \mathbf{p}_N)$  are the conjugate momenta.

TABLE I. Stability of one-dimensional conformations in the  $N$ -body chainlike bead-spring model under the equal masses and the identical springs. Column 2 lists the conformations  $c$ . The mode number is defined in ascending order of the eigenfrequencies. The stability of a conformation with a given mode is indicated by S (stable), Z (zero), and U (unstable) and the number after S, Z, and U represents the number of stable, zero, and unstable eigenvalues of  $D_\phi \mathbf{G}$ , respectively. After the slash, the value of  $(m/k)\omega_j^2$  is shown, where  $\omega_j$  is the eigenfrequency of the mode. Sequences of +, 0, and - represent the eigenmode symbol  $s$ . See the text for the definitions of  $c$  and  $s$ .

$N$	Conformation $c$	Stability/Square of eigenfrequency				
		Mode 1	Mode 2	Mode 3	Mode 4	Mode 5
3		S1/1	U1/3			
	(1)	(+, +)	(+, -)			
	(-1)	(+, -)	(+, +)			
4		S2/0.585786	Z2/2	U2/3.41421		
	(1,1)	(+, +, +)	(+, 0, -)	(+, -, +)		
	(1, -1)	(+, +, -)	(+, 0, +)	(+, -, -)		
	(-1, -1)	(+, -, +)	(+, 0, -)	(+, +, +)		
5		S3/0.381966	S2U1/1.38197	S1U2/2.61803	U3/3.61803	
	(1,1,1)	(+, +, +, +)	(+, +, -, -)	(+, -, -, +)	(+, -, +, -)	
	(1, 1, -1)	(+, +, +, -)	(+, +, -, +)	(+, -, -, -)	(+, -, +, +)	
	(1, -1, 1)	(+, +, -, -)	(+, +, +, +)	(+, -, +, -)	(+, -, -, +)	
	(1, -1, -1)	(+, +, -, +)	(+, +, +, -)	(+, -, +, +)	(+, -, -, -)	
	(-1, 1, -1)	(+, -, -, +)	(+, -, +, -)	(+, +, +, +)	(+, +, -, -)	
	(-1, -1, -1)	(+, -, +, -)	(+, -, -, +)	(+, +, -, -)	(+, +, +, +)	
6		S4/0.267949	S2Z2/1	Z4/2	Z2U2/3	U4/3.73205
	(1,1,1,1)	(+, +, +, +, +)	(+, +, 0, -, -)	(+, 0, -, 0, +)	(+, -, 0, +, -)	(+, -, +, -, +)
	(1, 1, 1, -1)	(+, +, +, +, -)	(+, +, 0, -, +)	(+, 0, -, 0, -)	(+, -, 0, +, +)	(+, -, +, -, -)
	(1, 1, -1, 1)	(+, +, +, -, -)	(+, +, 0, +, +)	(+, 0, -, 0, -)	(+, -, 0, -, +)	(+, -, +, +, -)
	(1, 1, -1, -1)	(+, +, +, -, +)	(+, +, 0, +, -)	(+, 0, -, 0, +)	(+, -, 0, -, -)	(+, -, +, +, +)
	(1, -1, 1, 1)	(+, +, -, -, -)	(+, +, 0, +, +)	(+, 0, +, 0, -)	(+, -, 0, -, +)	(+, -, -, +, -)
	(1, -1, 1, -1)	(+, +, -, -, +)	(+, +, 0, +, -)	(+, 0, +, 0, +)	(+, -, 0, -, -)	(+, -, -, +, +)
	(1, -1, -1, 1)	(+, +, -, +, +)	(+, +, 0, -, -)	(+, 0, +, 0, +)	(+, -, 0, +, -)	(+, -, -, -, +)
	(1, -1, -1, -1)	(+, +, -, +, -)	(+, +, 0, -, +)	(+, 0, +, 0, -)	(+, -, 0, +, +)	(+, -, -, -, -)
	(-1, 1, 1, -1)	(+, -, -, -, +)	(+, -, 0, +, -)	(+, 0, +, 0, +)	(+, +, 0, -, -)	(+, +, -, +, +)
	(-1, 1, -1, -1)	(+, -, -, +, -)	(+, -, 0, -, +)	(+, 0, +, 0, -)	(+, +, 0, +, +)	(+, +, -, -, -)
	(-1, -1, -1, -1)	(+, -, +, -, +)	(+, -, 0, +, -)	(+, 0, -, 0, +)	(+, +, 0, -, -)	(+, +, +, +, +)

The canonical equations of motion are

$$\frac{d\mathbf{r}_i}{dt} = \frac{\partial H}{\partial \mathbf{p}_i}, \quad \frac{d\mathbf{p}_i}{dt} = -\frac{\partial H}{\partial \mathbf{r}_i}, \quad i = 1, \dots, N. \quad (35)$$

### A. Potential energy

The theory includes the spring potential  $V_{\text{spring}}$  up to the quadratic order, and we use linear springs. The spring potential  $V_{\text{spring}}$  is

$$V_{\text{spring}}(\mathbf{r}) = \sum_{i=1}^{N-1} \frac{k}{2} (\|\mathbf{r}_{i+1} - \mathbf{r}_i\| - l_*)^2. \quad (36)$$

The bending potential  $U_{\text{bend}}$  is defined as

$$U_{\text{bend}}(\mathbf{r}) = \sum_{i<j} U_{\text{LJ}}(\|\mathbf{r}_j - \mathbf{r}_i\|) \quad (37)$$

and  $U_{\text{LJ}}$  is the Lennard-Jones potential

$$U_{\text{LJ}}(r) = 4\epsilon_{\text{LJ}} \left[ \left( \frac{\sigma}{r} \right)^{12} - \left( \frac{\sigma}{r} \right)^6 \right], \quad \epsilon_{\text{LJ}} = \epsilon^2, \quad \sigma = \frac{l_*}{2^{1/6}}. \quad (38)$$

The value of  $\sigma$  is determined so that the minimum point of  $U_{\text{LJ}}$  coincides with  $l_* = 1$  [see Eq. (33)] as shown in Fig. 4(a).

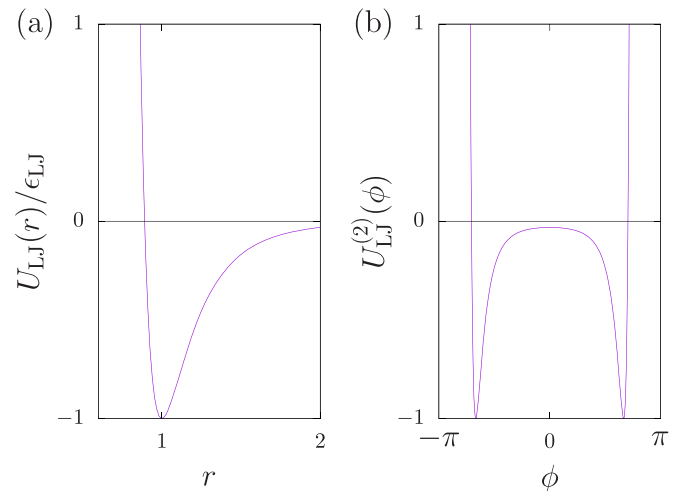


FIG. 4. Lennard-Jones potential: (a)  $U_{\text{LJ}}(r)/\epsilon_{\text{LJ}}$  [Eq. (38)] and (b)  $U_{\text{LJ}}^{(2)}(\phi)$  in  $N = 3$  [Eq. (39)].

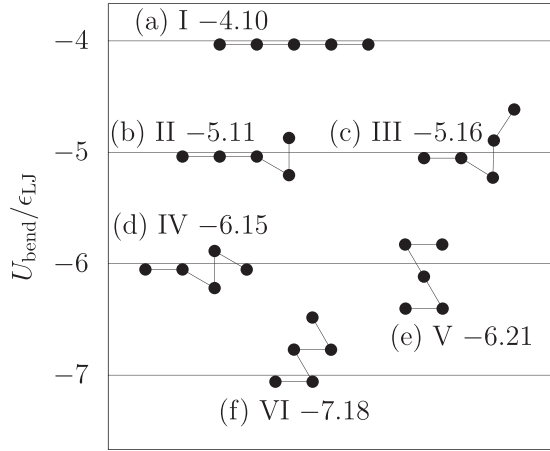


FIG. 5. Six conformations satisfying  $\nabla_{\phi} U_{\text{bend}}^{(2)}(\phi) = \mathbf{0}$ , labeled I–VI as indicated in the figure. The arabic numbers represent the scaled bending potential energy  $U_{\text{bend}}/\epsilon_{\text{LJ}}$ . The stability indices for  $E_{\text{normal}}^{(2)\text{ini}} = 0$  (i.e., based on  $U_{\text{bend}}$ ) are U3 (conformation I), S1U2 (II and III), S2U1 (IV and V), and S3 (VI). See the caption of Table I for the stability index.

For a guide, we show the second-order Lennard-Jones potential  $U_{\text{LJ}}^{(2)}$  between the first and third beads in  $N = 3$ . The potential depends on the bending angle  $\phi$  as

$$U_{\text{LJ}}^{(2)}(\phi) = 4 \left[ \left( \frac{\sigma^2}{2l_*^2(1 + \cos \phi)} \right)^6 - \left( \frac{\sigma^2}{2l_*^2(1 + \cos \phi)} \right)^3 \right]. \quad (39)$$

It takes the minimum value  $-1$  at  $\pm\phi_{\text{min}}$ , where

$$\phi_{\text{min}} = \left| \cos^{-1} \left[ \left( \frac{\sigma}{2^{1/3}l_*} \right)^2 - 1 \right] \right| = \frac{2\pi}{3}. \quad (40)$$

[See Fig. 4(b).] Clearly, a straight joint ( $\phi = 0$ ) induces instability and a bent joint ( $\phi = \pm\phi_{\text{min}}$ ) is stable.

### B. Initial conditions

The initial positions are determined by the spring lengths  $l$  and the bending angles  $\phi$  and we set them in the following three steps. In the first step, the spring lengths are set as the natural lengths:  $l = l_*$ . In the second step, we compute states satisfying  $\nabla_{\phi} U_{\text{bend}}^{(2)}(\phi) = \mathbf{0}$ , where  $\nabla_{\phi}$  is the gradient with respect to  $\phi$ . A stationary state can be computed by using the Newton-Raphson method for the vector field  $\nabla_{\phi} U_{\text{bend}}^{(2)}$  and picking up an initial trial from the six one-dimensional conformations reported in Fig. 3. We obtained six stationary conformations for  $U_{\text{bend}}^{(2)}$ , reported in Fig. 5, which we call conformations I–VI and denote them by  $\phi^{\text{I}}, \dots, \phi^{\text{VI}}$ . The initial bending angle vector  $\phi$  is set as one of them. In the third step, we modify the positions determined in the first and second steps to excite normal modes in a desired manner. For example, in conformation I, mode 1 is excited by adding a vector which is parallel to the first column vector of the diagonalizing matrix  $\mathbf{P}(l_*, \phi^{\text{I}})$  to conformation  $(l_*, \phi^{\text{I}})$ .

The initial momenta are zero for the horizontal direction of Fig. 5. For the vertical direction, we add perturbation to escape

from a stationary state: Each momentum value is drawn from the uniform distribution on the interval  $[-\epsilon^2, \epsilon^2]$ . The initial kinetic energy is of  $O(\epsilon^4)$ , and from Eq. (25) we have the relation up to  $O(\epsilon^2)$ ,

$$E^{(2)} - U_{\text{bend}}^{(2)}(\phi^x) = E_{\text{normal}}^{(2)\text{ini}}, \quad x \in \{\text{I}, \dots, \text{VI}\}. \quad (41)$$

We will investigate the stability of a conformation  $\phi^x$  by varying the initial value of  $E_{\text{normal}}^{(2)\text{ini}}$ .

### C. Dynamical stabilization

We excite mode 1 to induce the dynamical stabilization. Conformation I is an ideal subject for examinations (i) and (ii): Conformation  $\phi^{\text{I}}$  satisfies  $\mathbf{G}(\phi^{\text{I}}) = \mathbf{0}$  for any  $E_{\text{normal}}^{(2)\text{ini}} \geq 0$  since  $\phi^{\text{I}}$  is a one-dimensional conformation and  $\mathcal{T}_s(\phi^{\text{I}}) = 0$  [see Eqs. (C5) and (D2)]. The threshold of  $E_{\text{normal}}^{(2)\text{ini}}$  at which stability changes is predicted theoretically by computing the eigenvalues of the Jacobian matrix  $D_{\phi} \mathbf{G}(\phi^{\text{I}})$ . Objective (iii) is realized by investigating conformation II in detail, since  $\phi^{\text{II}}$  is no longer stationary and  $\mathbf{G}(\phi^{\text{II}}) \neq \mathbf{0}$  for  $E_{\text{normal}}^{(2)\text{ini}} > 0$ . Conformations III–V will be reported briefly and VI is skipped because of its native stability.

The stabilization is monitored by computing the average amplitude of  $\phi$ , defined by

$$\phi_{\text{amp}} = \frac{1}{N-2} \sum_{i=1}^{N-2} \left[ \max_{t \in [0, T]} \phi_i(t) - \min_{t \in [0, T]} \phi_i(t) \right]. \quad (42)$$

A stabilized conformation takes  $\phi_{\text{amp}} \simeq 0$ , while a fully flexible conformation takes  $\phi_{\text{amp}} \simeq 2\phi_{\text{min}} = 4\pi/3$ , which is the distance between the two minima of  $U_{\text{LJ}}^{(2)}$  [see Fig. 4(b)]. The validity of the hypothesis (17) is examined by observing temporal evolution of  $E_i^{(2)}/E_{\text{normal}}^{(2)}$  [see Eq. (C7) to compute  $E_i^{(2)}$ ].

The stabilization of conformation I is reported in Fig. 6(a). The amplitude  $\phi_{\text{amp}}$  drastically decreases at the theoretically obtained threshold of  $E_{\text{normal}}^{(2)\text{ini}}$ . The threshold is also confirmed from temporal evolution of  $\phi_i(t)$  reported in Figs. 6(b) and 6(c). Examination (i) is successfully performed in this example. The hypothesis (16) is satisfied on the stable side [Fig. 6(e)], while it is not satisfied in a long-time regime on the unstable side [Fig. 6(d)]. However, even on the unstable side, the normal mode energy ratios are almost constant in a short time regime ( $t < 3000$ ) and the theoretical prediction of instability is justified. Examination (ii) is then complete.

For examination (iii), conformation II is investigated in Fig. 7. The theoretical prediction of the stability change based on  $D_{\phi} \mathbf{G}(\phi^{\text{II}})$  is not as precise as observed in Fig. 7(a), since  $\phi^{\text{II}}$  is not stationary in the vector field  $\mathbf{G}$  for  $E_{\text{normal}}^{(2)\text{ini}} > 0$ . Nevertheless, excitation of the lowest-frequency normal mode stabilizes conformation  $\phi^{\text{II}}$ : The amplitude  $\phi_{\text{amp}}$  for  $T = 3000$  decreases as  $E_{\text{normal}}^{(2)\text{ini}}$  increases. The stabilization in a short-time regime is confirmed directly in Figs. 7(b) and 7(c). The hypothesis (16) is also approximately verified in Figs. 7(d) and 7(e). The dynamical stabilization breaks in a long-time regime, in which the Arnold diffusion [35] possibly kicks in and moves the bending angles far from their initial values.

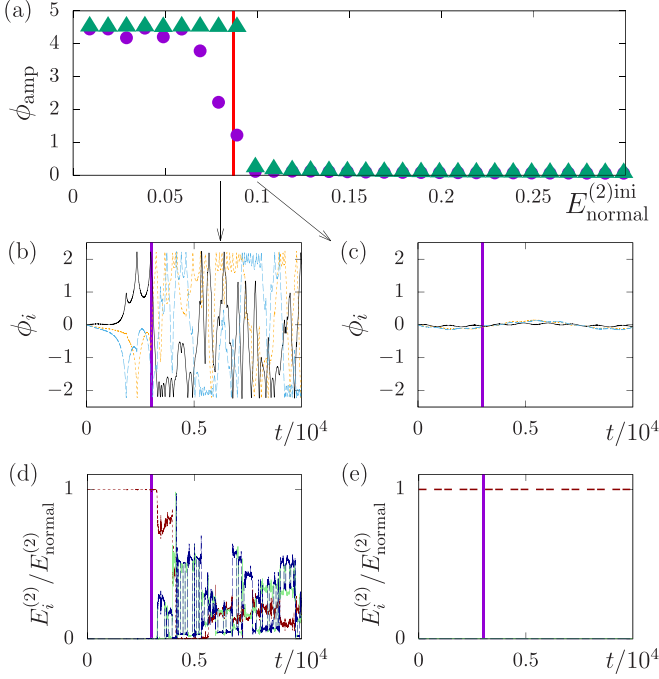


FIG. 6. Dynamical stabilization of conformation I. (a) Amplitude of the bending angles as a function of  $E_{\text{normal}}^{(2)\text{ini}}$ . The averaged time  $T$  is  $T = 3 \times 10^3$  (purple circles) and  $T = 3 \times 10^4$  (green triangles). The red vertical line at  $E_{\text{normal}}^{(2)\text{ini}} = 0.087$  is the theoretical prediction of the stability threshold. The temporal evolution of  $\phi_1$  (orange short-dashed line),  $\phi_2$  (black solid line), and  $\phi_3$  (light blue long-dashed line) is shown at (b)  $E_{\text{normal}}^{(2)\text{ini}} \simeq 0.08$  and (c)  $E_{\text{normal}}^{(2)\text{ini}} \simeq 0.10$ . The vertical purple line marks  $t = 3 \times 10^3$ . The temporal evolution of  $E_i^{(2)}/E_{\text{normal}}^{(2)}$  for  $i = 1$  (dark red short-dashed line),  $i = 2$  (green solid line), and  $i = 3$  (dark blue long-dashed line) is shown at (d)  $E_{\text{normal}}^{(2)\text{ini}} \simeq 0.08$  and (e)  $E_{\text{normal}}^{(2)\text{ini}} \simeq 0.10$ . In (e) the lines for  $i = 2$  and  $3$  are hard to see because they almost coincide with the zero-level line.

Stabilization of conformations III–V is summarized in Fig. 8. The amplitude  $\phi_{\text{amp}}$  tends to decrease as  $E_{\text{normal}}^{(2)\text{ini}}$  increases, and the theoretically obtained thresholds are approximately in good agreement with numerical observation of conformations IV and V.

#### D. Excited mode dependence

Let us examine the mode dependence of stability in conformation I. We fix the observation time as  $T = 10^4$ . The phase amplitude  $\phi_{\text{amp}}$  is reported in Fig. 9 by varying the excited mode. Mode 1 stabilizes conformation I as observed in Fig. 6, and as the theory predicts, the three other modes cannot stabilize it even if we increase the initial normal mode energy  $E_{\text{normal}}^{(2)\text{ini}}$ .

Next, to observe stabilization by a mixed mode, we excite modes 1 and 2 with the energy ratios  $\nu_1 \in [0, 1]$  and  $\nu_2 = 1 - \nu_1$ , respectively. The phase amplitude is shown in Fig. 10 as a function of  $\nu_1$  with the theoretically computed instability index, which is the number of unstable eigenvalues of  $D_\phi \mathbf{G}(\phi^1)$ . We confirm two facts: (i) DIC is robust whereas a destabilizing mode 2 is excited ( $\nu_2 = 1 - \nu_1 > 0$ ) and (ii) the amplitude is close to 0 if the theoretically computed instability

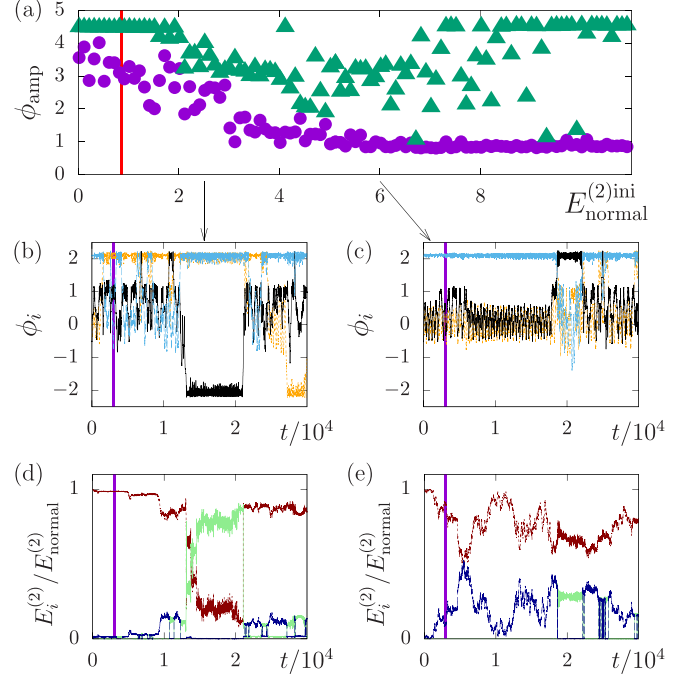


FIG. 7. Same as Fig. 6 but for conformation II for (b) and (d)  $E_{\text{normal}}^{(2)\text{ini}} \simeq 2.5$  and (c) and (e)  $E_{\text{normal}}^{(2)\text{ini}} \simeq 6.0$ .

index is 0. Large amplitudes around  $\nu_1 \lesssim 0.4$  where the instability index is zero can be explained as follows: Conformation I is stable but the stability is weak, and hence the system can escape from conformation I by a perturbation.

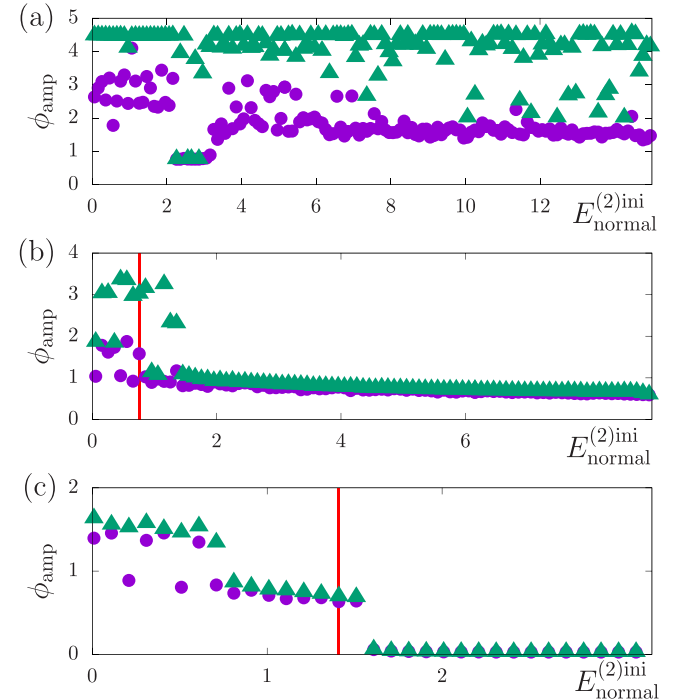


FIG. 8. Dynamical stabilization of conformations (a) III, (b) IV, and (c) V. The theoretical threshold represented by the vertical red solid line is not obtained in the reported interval of  $E_{\text{normal}}^{(2)\text{ini}}$  in (a).

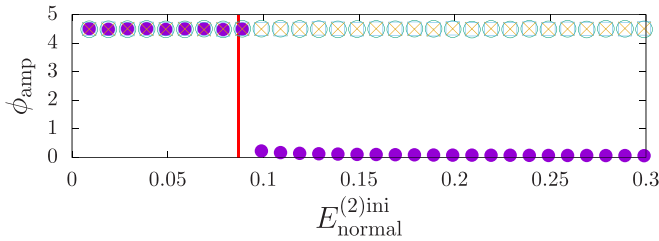


FIG. 9. Phase amplitude  $\phi_{\text{amp}}$  as a function of the initial normal mode energy  $E_{\text{normal}}^{(2)\text{ini}}$ . The average time is  $T = 10^4$ . The excited modes are mode 1 (purple closed circles), mode 2 (green open circles), mode 3 (blue squares), and mode 4 (orange crosses). The vertical red line is the theoretical threshold for mode 1.

## VI. SUMMARY

We have extended a theory of the dynamically induced conformation to  $N$ -body chainlike bead-spring models, while DIC was developed for  $N = 3$  in a previous work [20]. The theory predicts that the dynamical stability depends on the excited normal modes of the springs and on the normal mode energy.

As the simplest case we have studied a system without the bending potential to clearly exhibit dynamical effects. Concentrating on the so-called one-dimensional conformations, which are stationary, we have investigated the mode-dependent stability up to  $N = 6$  under the condition of equal masses and identical springs. Simple rules of the mode dependence have been discovered: A conformation is stabilized by exciting the lowest-eigenfrequency mode and destabilization emerges as the eigenfrequency of the excited normal mode becomes higher.

We stress that DIC is ubiquitous. The theory is also applicable for mixed modes, and the stabilization of a conformation is realized with an approximate probability of 0.8 up to  $N = 5$ , when we choose a mixed mode randomly. The probability 0.8 is notable because, among four normal modes in  $N = 5$ , only one mode contributes to the stabilization and the other three modes contribute to the destabilization. Moreover, the uniform setting of the equal masses and the identical springs is not essential for DIC [20]. It might be expected that a small dissipation does not break the theory developed in this article, because the (de)stabilization mechanism is based on separation of timescales. An examination has to be done.

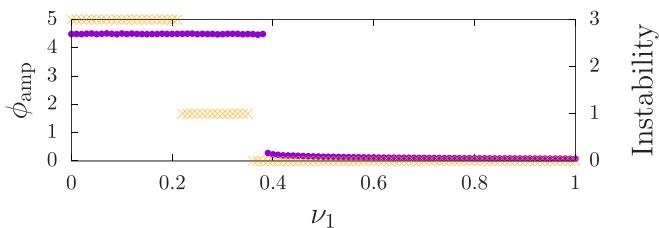


FIG. 10. Phase amplitude  $\phi_{\text{amp}}$  (purple circles) as a function of the initial normal mode energy ratio  $\nu_1$  of mode 1. The remaining energy is given to mode 2:  $\nu_2 = 1 - \nu_1$ . The average time is  $T = 10^4$ . The instability index (the right vertical axis) is shown by orange crosses.

The dynamical stabilization of conformations has been demonstrated numerically in a system having the bending potential consisting of the Lennard-Jones potentials for each pair of beads. As the theory predicts, any quasistationary conformation can be stabilized by exciting the lowest-eigenfrequency mode which depends on the conformation. It is worth noting that the Lennard-Jones potential takes a local maximum at a straight joint, but the straight conformation is stabilized by exciting normal modes.

Excitation of a normal mode is a nonequilibrium phenomenon, because the law of equipartition of energy breaks among the normal modes. Nevertheless, separation of the two timescales suggests that the importance of DIC survives in a long time by the Boltzmann-Jeans conjecture [36–42]. An important message of DIC is that the conformation is not determined by the bending potential only, and we have to input the dynamical (de)stabilization. This message sheds light on a different aspect of conformation and conformation change.

## ACKNOWLEDGMENTS

The author thanks T. Yanagita, T. Konishi, and M. Toda for valuable discussions. The author acknowledges the support of JSPS KAKENHI Grants No. JP16K05472 and No. JP21K03402.

## APPENDIX A: SUPPLEMENTS TO THE THEORY

We derive the Lagrangian (4) in Appendix A 1 and the equations of slow motion (19) in Appendix A 2.

### 1. Lagrangian in the internal coordinates

The Lagrangian in Cartesian coordinates is

$$L(\mathbf{r}, \dot{\mathbf{r}}) = K(\dot{\mathbf{r}}) - V(\mathbf{r}), \quad (\text{A1})$$

where the kinetic energy is

$$K(\dot{\mathbf{r}}) = \frac{1}{2} \sum_{i,j=1}^N M^{ij} \dot{\mathbf{r}}_i \cdot \dot{\mathbf{r}}_j \quad (\text{A2})$$

and

$$\mathbf{M} = \text{diag}(m_1, \dots, m_N). \quad (\text{A3})$$

We derive the Lagrangian (4) in the internal coordinates through three changes of variables: (i) the relative coordinates  $\mathbf{q}_i = \mathbf{r}_{i+1} - \mathbf{r}_i$ , (ii) the polar coordinates of  $\mathbf{q}_i$ , and (iii) the relative angles  $\phi_i$  between  $\mathbf{q}_{i+1}$  and  $\mathbf{q}_i$ . For simplicity of notation, we will omit the symbol of transposition for vectors as  $\mathbf{y} = (\mathbf{l}, \boldsymbol{\phi})$  if no confusion occurs.

The first change of variables from  $\mathbf{r}$  to  $\mathbf{q} = (\mathbf{q}_1, \dots, \mathbf{q}_N)$  is performed as

$$\begin{pmatrix} \mathbf{q}_1 \\ \vdots \\ \mathbf{q}_N \end{pmatrix} = \mathbf{S}_M \begin{pmatrix} \mathbf{r}_1 \\ \vdots \\ \mathbf{r}_N \end{pmatrix}, \quad (\text{A4})$$

where the matrix  $\mathbf{S}_M \in \text{Mat}(N)$  is defined by

$$\mathbf{S}_M = \begin{pmatrix} -1 & 1 & 0 & \cdots & 0 & 0 \\ 0 & -1 & 1 & \ddots & 0 & 0 \\ 0 & 0 & -1 & \ddots & 0 & 0 \\ \vdots & \ddots & \ddots & \ddots & \ddots & \vdots \\ 0 & 0 & 0 & \cdots & -1 & 1 \\ m_1/M & m_2/M & m_3/M & \cdots & m_{N-1}/M & m_N/M \end{pmatrix} \quad (\text{A5})$$

and

$$M = \text{Tr } \mathbf{M} = \sum_{i=1}^N m_i. \quad (\text{A6})$$

The last element  $q_N$  is a cyclic coordinate corresponding to the total momentum conservation due to the translational symmetry. We set the total momentum as zero and neglect the last element.

The second change of variables introduces the polar coordinates to  $\mathbf{q}_i$ . We denote the length and the argument of  $\mathbf{q}_i$  by  $l_i$  and  $\theta_i$ , respectively.

The third change of variables from  $\boldsymbol{\theta} = (\theta_1, \dots, \theta_{N-1})$  to  $\boldsymbol{\phi} = (\phi_1, \dots, \phi_{N-1})$  is performed as  $\boldsymbol{\phi} = \mathbf{S}\boldsymbol{\theta}$ , where

$$\mathbf{S} = \begin{pmatrix} -1 & 1 & 0 & \cdots & 0 & 0 \\ 0 & -1 & 1 & \ddots & 0 & 0 \\ 0 & 0 & -1 & \ddots & 0 & 0 \\ \vdots & \ddots & \ddots & \ddots & \ddots & \vdots \\ 0 & 0 & 0 & \cdots & -1 & 1 \\ \frac{1}{N-1} & \frac{1}{N-1} & \frac{1}{N-1} & \cdots & \frac{1}{N-1} & \frac{1}{N-1} \end{pmatrix} \in \text{Mat}(N-1). \quad (\text{A7})$$

The last element  $\phi_{N-1}$  is a cyclic coordinate corresponding to the total angular momentum conservation due to the rotational symmetry. We keep it for simplicity of computations.

Finally, we obtain the kinetic energy in the internal coordinates  $\mathbf{y} = (\mathbf{l}, \boldsymbol{\phi})$  as

$$K(\mathbf{y}, \dot{\mathbf{y}}) = \frac{1}{2} \dot{\mathbf{y}}^T \mathbf{B}(\mathbf{y}) \dot{\mathbf{y}}, \quad (\text{A8})$$

where

$$\mathbf{B}(\mathbf{y}) = \begin{pmatrix} \mathbf{B}_{ll}(\boldsymbol{\phi}) & \mathbf{B}_{l\phi}(\mathbf{y}) \\ \mathbf{B}_{\phi l}(\mathbf{y}) & \mathbf{B}_{\phi\phi}(\mathbf{y}) \end{pmatrix} \in \text{Mat}(2N-2) \quad (\text{A9})$$

and the submatrices of size  $N-1$  are

$$\begin{pmatrix} \mathbf{B}_{ll} & \mathbf{B}_{l\phi} \\ \mathbf{B}_{\phi l} & \mathbf{B}_{\phi\phi} \end{pmatrix} = \begin{pmatrix} \mathbf{A}_C(\boldsymbol{\phi}) & \mathbf{A}_S(\boldsymbol{\phi})\mathbf{L}\mathbf{S}^{-1} \\ -\mathbf{S}^{-T}\mathbf{L}\mathbf{A}_S(\boldsymbol{\phi}) & \mathbf{S}^{-T}\mathbf{L}\mathbf{A}_C(\boldsymbol{\phi})\mathbf{L}\mathbf{S}^{-1} \end{pmatrix}. \quad (\text{A10})$$

The matrix  $\mathbf{L}$  is diagonal and defined by

$$\mathbf{L}(\mathbf{l}) = \text{diag}(l_1, \dots, l_{N-1}). \quad (\text{A11})$$

The  $(i, j)$  elements of the matrices  $\mathbf{A}_C$  and  $\mathbf{A}_S$  are

$$A_C^{ij} = A^{ij} \cos \phi_{i,j}, \quad A_S^{ij} = A^{ij} \sin \phi_{i,j}, \quad (\text{A12})$$

respectively, with

$$\phi_{i,j} = \begin{cases} \phi_j + \cdots + \phi_{i-1}, & i > j \\ 0, & i = j \\ -(\phi_i + \cdots + \phi_{j-1}), & i < j, \end{cases} \quad (\text{A13})$$

where the matrix  $\mathbf{A} \in \text{Mat}(N-1)$  is the upper left square block of size  $N-1$  of the matrix  $\mathbf{S}_M^{-T} \mathbf{M} \mathbf{S}_M^{-1} \in \text{Mat}(N)$ .

## 2. Averaged Euler-Lagrange equations in $O(\epsilon^2)$

In  $O(\epsilon^2)$  the Euler-Lagrange equations are

$$B^{\alpha\beta}(\mathbf{y}^{(0)}) (\ddot{y}_\beta)^{(2)} + D_\alpha^{\beta\gamma}(\mathbf{y}^{(0)}) (\dot{y}_\beta)^{(1)} (\dot{y}_\gamma)^{(1)} + \frac{\partial B^{\alpha\beta}}{\partial y_\gamma}(\mathbf{y}^{(0)}) (\dot{y}_\beta)^{(1)} y_\gamma^{(1)} + \frac{\partial U_{\text{bend}}^{(2)}}{\partial y_\alpha}(\mathbf{y}^{(0)}) = 0, \quad (\text{A14})$$

where

$$D_\alpha^{\beta\gamma}(\mathbf{y}) = \frac{\partial B^{\alpha\beta}}{\partial y_\gamma}(\mathbf{y}) - \frac{1}{2} \frac{\partial B^{\beta\gamma}}{\partial y_\alpha}(\mathbf{y}) \quad (\text{A15})$$

and

$$\begin{aligned} (\dot{\mathbf{y}})^{(1)} &= \frac{d\mathbf{y}^{(0)}}{dt_1} + \frac{\partial \mathbf{y}^{(1)}}{\partial t_0}, & (\ddot{\mathbf{y}})^{(1)} &= \frac{\partial^2 \mathbf{y}^{(1)}}{\partial t_0^2}, \\ (\ddot{\mathbf{y}})^{(2)} &= \frac{d^2 \mathbf{y}^{(0)}}{dt_1^2} + 2 \frac{\partial^2 \mathbf{y}^{(1)}}{\partial t_0 \partial t_1}. \end{aligned} \quad (\text{A16})$$

The vector  $(\dot{\mathbf{y}})^{(1)}$  is the first-order part of  $\dot{\mathbf{y}}$  and  $(\dot{\mathbf{y}})^{(1)} \neq d\mathbf{y}^{(1)}/dt$ .

Performing the averaging over the fast timescale  $t_0$ , which is denoted by  $\langle \cdots \rangle$ , we have

$$\begin{aligned} B^{\alpha\beta}(\mathbf{y}^{(0)}) \frac{d^2 y_\beta^{(0)}}{dt_1^2} + D_\alpha^{\beta\gamma}(\mathbf{y}^{(0)}) \frac{d y_\beta^{(0)}}{dt_1} \frac{d y_\gamma^{(0)}}{dt_1} + \frac{\partial U_{\text{bend}}^{(2)}}{\partial y_\alpha}(\mathbf{y}^{(0)}) \\ = \frac{1}{2} \text{Tr} \left( \frac{\partial \mathbf{B}}{\partial y_\alpha}(\mathbf{y}^{(0)}) \mathbf{X}(\mathbf{y}^{(0)}) (\mathbf{y}^{(1)} \mathbf{y}^{(1)T}) \right). \end{aligned} \quad (\text{A17})$$

The right-hand side represents the effective force by the fast motion of normal modes. We use the relation

$$\left\langle \frac{\partial \mathbf{y}^{(1)}}{\partial t_0} \left( \frac{\partial \mathbf{y}^{(1)}}{\partial t_0} \right)^T \right\rangle = \mathbf{X}(\mathbf{y}^{(0)}) (\mathbf{y}^{(1)} \mathbf{y}^{(1)T}), \quad (\text{A18})$$

proven by the integration by parts. Substituting the solutions into Eq. (12), we have

$$\langle \mathbf{y}^{(1)} \mathbf{y}^{(1)T} \rangle = \frac{1}{2} \mathbf{P}(\mathbf{y}^{(0)}) \mathbf{W}^2 \mathbf{P}(\mathbf{y}^{(0)})^T, \quad (\text{A19})$$

where the diagonal matrix of size  $2N-2$ ,

$$\mathbf{W} = \text{diag}(w_1, \dots, w_{N-1}, 0, \dots, 0), \quad (\text{A20})$$

contains the amplitudes  $\mathbf{w}$  of the normal modes.

Focusing on the motion of  $\boldsymbol{\phi}^{(0)}(t_0)$ , we have the equations of motion

$$\begin{aligned} B_{\phi\phi}^{ij}(\mathbf{y}^{(0)}) \frac{d^2 \phi_j^{(0)}}{dt_1^2} + \left( \frac{\partial B_{\phi\phi}^{ij}}{\partial \phi_n} - \frac{1}{2} \frac{\partial B_{\phi\phi}^{jn}}{\partial \phi_i} \right) \frac{d\phi_j^{(0)}}{dt_1} \frac{d\phi_n^{(0)}}{dt_1} \\ + \frac{\partial U_{\text{bend}}^{(2)}}{\partial \phi_i}(\mathbf{y}^{(0)}) = \frac{1}{4} \text{Tr} \left( \frac{\partial \mathbf{B}}{\partial \phi_i} \mathbf{P} \mathbf{W}^2 \mathbf{P}^T \right) \end{aligned} \quad (\text{A21})$$

because of  $\mathbf{X}\mathbf{P} = \mathbf{P}\mathbf{A}$ . Finally, substituting the hypothesis (16), which is read as  $\mathbf{W}^2 = w(t_1)^2\mathbf{N}$ , and using the averaged energy (25), we have the equations of motion (19) for the slow bending motion  $\phi^{(0)}(t_1)$ .

### APPENDIX B: ORDERING OF THE POTENTIAL FUNCTION

We prove that the assumptions of Eqs. (6) and (8) induce Eq. (9). The potential  $V(\mathbf{y})$  is expanded into the power series of  $\epsilon$  as

$$V(\mathbf{y}) = V^{(0)}(\mathbf{y}) + \epsilon V^{(1)}(\mathbf{y}) + \epsilon^2 V^{(2)}(\mathbf{y}) + \dots \quad (\text{B1})$$

We show that  $V^{(0)}$  and  $V^{(1)}$  depend on only  $l$ , and hence

$$V_{\text{spring}}(\mathbf{l}) = V^{(0)}(\mathbf{l}) + \epsilon V^{(1)}(\mathbf{l}), \quad U_{\text{bend}}(\mathbf{y}) = \epsilon^2 V^{(2)}(\mathbf{y}) + \dots \quad (\text{B2})$$

Since  $\dot{\mathbf{y}}, \ddot{\mathbf{y}} = O(\epsilon)$ , the zeroth-order equations of motion are, for  $\alpha = 1, \dots, 2N - 2$ ,

$$\left( \frac{\partial V}{\partial y_\alpha}(\mathbf{y}) \right)^{(0)} = \frac{\partial V^{(0)}}{\partial y_\alpha}(\mathbf{l}_*, \phi^{(0)}) = 0, \quad (\text{B3})$$

where  $(A)^{(m)}$  extracts the  $O(\epsilon^m)$  terms of  $A$ . The above equality implies that  $V^{(0)}$  does not depend on  $\phi$ , since  $\phi^{(0)}$  is arbitrary. We denote it by  $V^{(0)}(\mathbf{l})$ .

The equations of motion in  $O(\epsilon)$  are

$$B^{\alpha\beta}(\mathbf{y}^{(0)}) \frac{\partial^2 y_\beta^{(1)}}{\partial t_0^2} + \frac{\partial^2 V^{(0)}}{\partial y_\alpha \partial y_\beta}(\mathbf{l}_*) y_\beta^{(1)} + \frac{\partial V^{(1)}}{\partial y_\alpha}(\mathbf{l}_*, \phi^{(0)}) = 0. \quad (\text{B4})$$

The second term on the left-hand side is the spring force. The third term is constant in the fast timescale  $t_0$  and it yields secular terms in  $\phi^{(1)}$ . The existence of the secular terms breaks the assumption (7) and the third term must be zero. Therefore,  $V^{(1)}$  depends on only  $l$  as  $V^{(0)}$ .

### APPENDIX C: SIMPLIFICATIONS

We can simplify the expressions of the functions  $\mathcal{T}_i$  and the spring energy, which help to analyze the stability of a stationary state. The idea is to decompose a size- $(2N - 2)$  matrix into four half-size submatrices. The inverse matrix  $\mathbf{B}^{-1}$  is decomposed into

$$\mathbf{B}^{-1} = \begin{pmatrix} \tilde{\mathbf{B}}_{ll} & \tilde{\mathbf{B}}_{l\phi} \\ \tilde{\mathbf{B}}_{\phi l} & \tilde{\mathbf{B}}_{\phi\phi} \end{pmatrix} \in \text{Mat}(2N - 2), \quad (\text{C1})$$

where

$$\begin{aligned} \tilde{\mathbf{B}}_{ll} &= (\mathbf{A}_C + \mathbf{A}_S \mathbf{A}_C^{-1} \mathbf{A}_S)^{-1}, \\ \tilde{\mathbf{B}}_{l\phi} &= -\mathbf{A}_C^{-1} \mathbf{A}_S \tilde{\mathbf{B}}_{ll} \mathbf{L}^{-1} \mathbf{S}^T, \\ \tilde{\mathbf{B}}_{\phi l} &= \mathbf{S} \mathbf{L}^{-1} \mathbf{A}_S^{-1} \mathbf{A}_S \tilde{\mathbf{B}}_{ll}, \\ \tilde{\mathbf{B}}_{\phi\phi} &= \mathbf{S} \mathbf{L}^{-1} \tilde{\mathbf{B}}_{ll} \mathbf{L}^{-1} \mathbf{S}^T. \end{aligned} \quad (\text{C2})$$

The matrix  $\mathbf{P}$ , which diagonalizes the matrix  $\mathbf{X} = \mathbf{B}^{-1} \mathbf{K}$ , is also decomposed into

$$\mathbf{P} = \begin{pmatrix} \mathbf{P}_l & \mathbf{O} \\ \mathbf{P}_\phi & \mathbf{E} \end{pmatrix} \in \text{Mat}(2N - 2), \quad (\text{C3})$$

where  $\mathbf{P}_l$  solves the eigenvalue problem  $(\tilde{\mathbf{B}}_{ll} \mathbf{K}_l) \mathbf{P}_l = \mathbf{P}_l \mathbf{A}_l$  and

$$\mathbf{P}_\phi = -\mathbf{B}_{\phi\phi}^{-1} \mathbf{B}_{\phi l} \mathbf{P}_l = \mathbf{S} \mathbf{L}^{-1} \mathbf{A}_C^{-1} \mathbf{A}_S \mathbf{P}_l. \quad (\text{C4})$$

The functions  $\mathcal{T}_i$  are simplified to

$$\mathcal{T}_i = \frac{\text{Tr}(\mathbf{P}_l^T \frac{\partial \tilde{\mathbf{B}}_{ll}^{-1}}{\partial \phi_i} \mathbf{P}_l \mathbf{A}_l \mathbf{N}_l)}{\text{Tr}(\mathbf{P}_l^T \mathbf{K}_l \mathbf{P}_l \mathbf{N}_l)}, \quad i = 1, \dots, N - 1. \quad (\text{C5})$$

Similarly, the averaged normal mode energy  $\langle E_{\text{normal}}^{(2)} \rangle$  is simplified as

$$\langle E_{\text{normal}}^{(2)} \rangle = \frac{1}{2} \text{Tr}(\mathbf{P}_l^T \mathbf{K}_l \mathbf{P}_l \mathbf{W}_l^2), \quad (\text{C6})$$

where  $\mathbf{W}_l = \text{diag}(w_1, \dots, w_{N-1})$ .

Temporal evolution of  $E_i^{(2)}$ , the contribution to  $E_{\text{normal}}^{(2)}$  from the  $i$ th mode, is computed as

$$E_i^{(2)} = \frac{1}{2} [\mathbf{P}_l^{-1} \mathbf{l}^{(1)}]_i^2 + \frac{1}{2\lambda_i} [\mathbf{P}_l^{-1} \dot{\mathbf{l}}^{(1)}]_i^2, \quad i = 1, \dots, N - 1. \quad (\text{C7})$$

Here  $[\mathbf{P}_l^{-1} \mathbf{l}^{(1)}]_i$  is the  $i$ th element of the vector  $\mathbf{P}_l^{-1} \mathbf{l}^{(1)}$ . We neglected the time derivative of  $\mathbf{P}_l^{-1}(\phi^{(0)}(t_1) + \epsilon \phi^{(1)}(t_0, t_1))$  since its contribution is higher than  $O(\epsilon^2)$ .

We can choose the matrix  $\mathbf{P}$  so that

$$\mathbf{Q}_l = \sqrt{\mathbf{K}_l} \mathbf{P}_l \in O(N - 1), \quad (\text{C8})$$

where  $O(n)$  is the set of real orthogonal matrices of size  $n$ . The square root  $\sqrt{\mathbf{K}_l}$  is well defined, since the real symmetric matrix  $\mathbf{K}_l$  is assumed to be positive definite. Choosing the above  $\mathbf{P}_l$ , we have  $\mathbf{P}_l^T \mathbf{K}_l \mathbf{P}_l = \mathbf{E}$ , which further simplifies  $\mathcal{T}_i$  ( $i = 1, \dots, N - 1$ ) and  $\langle E_{\text{normal}}^{(2)} \rangle$ .

### APPENDIX D: STATIONARITY AND STABILITY OF ONE-DIMENSIONAL CONFORMATIONS

We first note that

$$\mathbf{A}_S(\phi \in \mathcal{C}^1) = \frac{\partial \mathbf{A}_C}{\partial \phi_i}(\phi \in \mathcal{C}^1) = \mathbf{O}, \quad i = 1, \dots, N - 1, \quad (\text{D1})$$

because all the elements depend on  $\sin \phi_{i,j}$  in  $\mathbf{A}_S$  and  $\partial \mathbf{A}_C / \partial \phi_i$ , and  $\sin \phi_{i,j} = 0$  for a conformation belonging to  $\mathcal{C}^1$ . This fact implies that

$$\frac{\partial \tilde{\mathbf{B}}_{ll}^{-1}}{\partial \phi_i}(\phi \in \mathcal{C}^1) = \left( \frac{\partial \mathbf{A}_C}{\partial \phi_i} + \frac{\partial (\mathbf{A}_S \mathbf{A}_C^{-1} \mathbf{A}_S)}{\partial \phi_i} \right)_{\phi \in \mathcal{C}^1} = \mathbf{O} \quad (\text{D2})$$

and

$$\mathcal{T}_i(\phi \in \mathcal{C}^1) = 0 \quad (\text{D3})$$

for  $i = 1, \dots, N - 1$ . Thus, we have  $\mathbf{G}(\phi \in \mathcal{C}^1) = \mathbf{0}$  for  $U_{\text{bend}}^{(2)} \equiv 0$  from Eq. (21).

Similarly, the Jacobian matrix  $D_\phi \mathbf{G}$  is simplified as

$$\frac{\partial G_i}{\partial \phi_j}(\phi \in \mathcal{C}^1) = -\frac{E^{(2)}}{2} (B_{\phi\phi}^{-1})^{in} \frac{\text{Tr}(\mathbf{P}_l^T \mathbf{Y}_{nj} \mathbf{P}_l \mathbf{A}_l \mathbf{N}_l)}{\text{Tr}(\mathbf{P}_l \mathbf{K}_l \mathbf{P}_l \mathbf{N}_l)}, \quad (\text{D4})$$

where

$$\mathbf{Y}_{ij} = \frac{\partial^2 \mathbf{A}_C}{\partial \phi_i \partial \phi_j} + \frac{\partial \mathbf{A}_S}{\partial \phi_i} \mathbf{A}_C^{-1} \frac{\partial \mathbf{A}_S}{\partial \phi_j} + \frac{\partial \mathbf{A}_S}{\partial \phi_j} \mathbf{A}_C^{-1} \frac{\partial \mathbf{A}_S}{\partial \phi_i}. \quad (\text{D5})$$

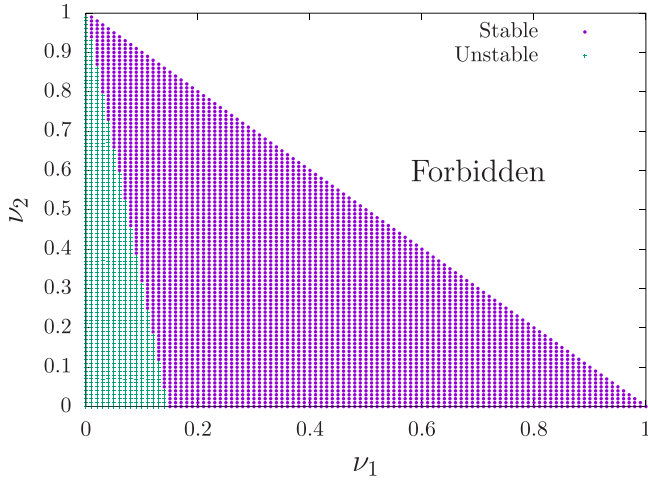


FIG. 11. Stable (purple circles) and unstable (green crosses) regions on the parameter plane  $(\nu_1, \nu_2)$  for  $N = 4$ . All the one-dimensional conformations share this diagram. The parameter  $\nu_3$  is determined by  $\nu_3 = 1 - \nu_1 - \nu_2$ . The critical point on the line  $\nu_2 = 0$  is  $\nu_{1c} \simeq 0.1464466$ .

We remark that each of  $\mathbf{Y}_{ij}$  ( $i, j = 1, \dots, N - 1$ ) is a size- $(N - 1)$  matrix. Further, the matrix  $\tilde{\mathbf{B}}_{ll}^{-1}$  is also simplified to

$$\tilde{\mathbf{B}}_{ll}^{-1}(\boldsymbol{\phi} \in \mathcal{C}^1) = \mathbf{A}_C(\boldsymbol{\phi} \in \mathcal{C}^1). \quad (\text{D6})$$

#### APPENDIX E: DYNAMICAL STABILITY OF ONE-DIMENSIONAL CONFORMATIONS BY MIXED MODES

Let the bending potential be absent:  $U_{\text{bend}} \equiv 0$ . We study the stability of a one-dimensional conformation with exciting multiple modes under the condition of equal masses and identical springs expressed in Eq. (27). The normal mode energy ratios  $\nu_i$  ( $i = 1, \dots, N - 1$ ) are set as

$$\text{Tr}\mathbf{N} = \sum_{i=1}^{N-1} \nu_i = 1, \quad 0 \leq \nu_i \leq 1, \quad (\text{E1})$$

and the number of the free parameters is  $N - 2$ . We compute the  $N$  dependence of the stable probability  $p_s(N)$  with which a considered one-dimensional conformation is stabilized by excited normal modes. Note that a conformation for  $U_{\text{bend}} \equiv 0$  is marginally stable and is easily modified, if no normal modes are excited.

A necessary and sufficient condition of the stability for  $N = 3$  is

$$\text{the conformation is stable} \iff \frac{1}{4} < \nu_1 \leq 1 \quad (\text{E2})$$

for conformations  $\mathbf{c} = (1)$  (straight) and  $\mathbf{c} = (-1)$  (bent). The condition implies that the probability is

$$p_s(3) = 0.75. \quad (\text{E3})$$

This stable probability for the two conformations is not a contradiction because multistability of the two conformations is realized in the interval  $\frac{1}{4} < \nu_1 < \frac{3}{4}$ . The condition of Eq. (E2) is in agreement with the conclusion reported previously [20], although the rotational symmetry is not reduced in the present theory while it is reduced in the previous theory.

For  $N = 4$ , we performed numerical computations of stability at the lattice points  $(n_1/100, n_2/100)$  ( $n_1, n_2 = 0, \dots, 100$ ) on the parameter plane  $(\nu_1, \nu_2)$ , where  $\nu_3$  is determined from Eq. (E1). The stable and unstable regions are reported in Fig. 11, which is shared by all one-dimensional conformations. The stability boundary is straight and the critical value  $\nu_{1c}$  on the line  $\nu_2 = 0$  is in the interval  $[0.1464466, 0.1464467]$ . The stable probability is thus

$$p_s(4) \simeq 0.8535. \quad (\text{E4})$$

The stability check on the lattice points is also performed on the parameter space  $(\nu_1, \nu_2, \nu_3)$  for  $N = 5$ . Among all 176851 researched points, the six conformations are stable at 141019 points. Thus, the stable probability is, for all the one-dimensional conformations,

$$p_s(5) \simeq 0.7974. \quad (\text{E5})$$

The probabilities  $p_s(3)$ ,  $p_s(4)$ , and  $p_s(5)$  suggest that dynamical stability is important even if the system size is large and multiple modes are excited.

- 
- [1] A. Stephenson, On induced stability, *Philos. Mag.* **15**, 233 (1908).
  - [2] P. L. Kapitza, Dynamic stability of a pendulum when its point of suspension vibrates, *Sov. Phys. JETP* **21**, 588 (1951); *Collected Papers of P. L. Kapitza*, edited by D. Ter Haar (Elsevier, Amsterdam, 1965), Vol. 2, pp. 714–725.
  - [3] E. I. Butikov, On the dynamic stabilization of an inverted pendulum, *Am. J. Phys.* **69**, 755 (2001).
  - [4] M. Bukov, L. D'Alessio, and A. Polkovnikov, Universal high-frequency behavior of periodically driven systems: From dynamical stabilization to Floquet engineering, *Adv. Phys.* **64**, 139 (2015).
  - [5] R. Citro, E. G. Dalla Torre, L. D'Alessio, A. Polkovnikov, M. Babadi, T. Oka, and E. Demler, Dynamical stability of a many-body Kapitza pendulum, *Ann. Phys. (NY)* **360**, 694 (2015).
  - [6] C. J. Richards, T. J. Smart, P. H. Jones, and D. Cubero, A microscopic Kapitza pendulum, *Sci. Rep.* **8**, 13107 (2018).
  - [7] J. F. Gloy, A. Siemens, and P. Schmelcher, Driven toroidal helix as a generalization of the Kapitza pendulum, *Phys. Rev. E* **105**, 054204 (2022).
  - [8] M. S. Krieger, Interfacial fluid instabilities and Kapitza pendula, *Eur. Phys. J. E* **40**, 67 (2017).
  - [9] B. Apffel, F. Novkoski, A. Eddi, and E. Fort, Floating under a levitating liquid, *Nature (London)* **585**, 48 (2020).
  - [10] R. E. Bellman, J. Bentsman, and S. M. Meerkov, Vibrational control of nonlinear systems, *IEEE Trans. Autom. Control* **31**, 710 (1986).
  - [11] B. Shapiro and B. T. Zinn, High-frequency nonlinear vibrational control, *IEEE Trans. Autom. Control* **42**, 83 (1997).

- [12] J. Martin, B. Georgeot, D. Guéry-Odelin, and D. L. Shepelyansky, Kapitza stabilization of a repulsive Bose-Einstein condensate in an oscillating optical lattice, *Phys. Rev. A* **97**, 023607 (2018).
- [13] V. S. Bagnato, N. P. Bigelow, G. I. Surdutovich, and S. C. Zilio, Dynamical stabilization: A new model for supermolasses, *Opt. Lett.* **19**, 1568 (1994).
- [14] R. J. Cook, D. G. Shankland, and A. L. Wells, Quantum theory of particle motion in a rapidly oscillating field, *Phys. Rev. A* **31**, 564 (1985).
- [15] S. Rahav, I. Gilary, and S. Fishman, Time Independent Description of Rapidly Oscillating Potentials, *Phys. Rev. Lett.* **91**, 110404 (2003).
- [16] S. Rahav, I. Gilary, and S. Fishman, Effective Hamiltonians for periodically driven systems, *Phys. Rev. A* **68**, 013820 (2003).
- [17] I. Gilary, N. Moiseyev, S. Rahav, and S. Fishman, Trapping of particles by lasers: The quantum Kapitza pendulum, *J. Phys. A: Math. Gen.* **36**, L409 (2003).
- [18] B. T. Torosov, G. Della Valle, and S. Longhi, Imaginary Kapitza pendulum, *Phys. Rev. A* **88**, 052106 (2013).
- [19] P. E. Rouse, Jr., A theory of the linear viscoelastic properties of dilute solutions of coiling polymers, *J. Chem. Phys.* **21**, 1272 (1953).
- [20] Y. Y. Yamaguchi, T. Yanagita, T. Konishi, and M. Toda, Dynamically induced conformation depending on excited normal modes of fast oscillation, *Phys. Rev. E* **105**, 064201 (2022).
- [21] T. Yanagita and T. Konishi, Numerical analysis of new oscillatory mode of bead-spring model, *Jpn. J. Soc. Civil Eng. A2* **75**, L\_125 (2019).
- [22] C. M. Bender and S. A. Orszag, *Advanced Mathematical Methods for Scientists and Engineers I: Asymptotic Methods and Perturbation Theory* (Springer, Berlin, 1999).
- [23] N. M. Krylov and N. N. Bogoliubov, *New Methods of Nonlinear Mechanics in their Application to the Investigation of the Operation of Electronic Generators. I* (United Scientific and Technical Press, Moscow, 1934).
- [24] N. M. Krylov and N. N. Bogoliubov, *Introduction to Nonlinear Mechanics* (Princeton University Press, Princeton, 1947).
- [25] J. Guckenheimer and P. Holmes, *Nonlinear Oscillations, Dynamical Systems, and Bifurcations of Vector Fields* (Springer, New York, 1983).
- [26] T. Yanao and K. Takatsuka, Collective coordinates and an accompanying metric force in structural isomerization dynamics of molecules, *Phys. Rev. A* **68**, 032714 (2003).
- [27] T. Yanao and K. Takatsuka, Kinematic effects associated with molecular frames in structural isomerization dynamics of clusters, *J. Chem. Phys.* **120**, 8924 (2004).
- [28] T. Yanao and K. Takatsuka, Effects of an intrinsic metric of molecular internal space on chemical reaction dynamics, in *Geometric Structures of Phase Space in Multidimensional Chaos A Special Volume of Advanced in Chemical Physics, Part B*, edited by M. Toda, T. Komatsuzaki, T. Konishi, R. S. Berry, and S. A. Rice (Wiley, New Jersey, 2005), Vol. 130, pp. 87–128.
- [29] T. Yanao, W. S. Koon, J. E. Marsden, and I. G. Kevrekidis, Gyration-radius dynamics in structural transitions of atomic clusters, *J. Chem. Phys.* **126**, 124102 (2007).
- [30] B. C. Dian, A. Longarte, and T. S. Zwier, Conformational dynamics in a dipeptide after single-mode vibrational excitation, *Science* **296**, 2369 (2002).
- [31] O. K. Rice and H. C. Ramsperger, Theories of unimolecular gas reactions at low pressures, *J. Am. Chem. Soc.* **49**, 1617 (1927).
- [32] L. S. Kassel, Studies in homogeneous gas reactions I, *J. Phys. Chem.* **32**, 225 (1928).
- [33] R. A. Marcus, Unimolecular dissociations and free radical recombination reactions, *J. Chem. Phys.* **20**, 359 (1952).
- [34] H. Yoshida, Construction of higher order symplectic integrators, *Phys. Lett. A* **150**, 262 (1990).
- [35] V. I. Arnold, Instability of dynamical systems with several degrees of freedom, *Sov. Math. Dokl.* **5**, 581 (1964).
- [36] D. D. Holm, J. E. Marsden, T. Ratiu, and A. Weinstein, Non-linear stability of fluid and plasma equilibria, *Phys. Rep.* **123**, 1 (1985).
- [37] L. Boltzmann, On certain questions of the theory of gases, *Nature (London)* **51**, 413 (1895).
- [38] J. H. Jeans, On the vibrations set up in molecules by collisions, *Philos. Mag.* **6**, 279 (1903).
- [39] J. H. Jeans, On the partition of energy between matter and aether, *Philos. Mag.* **10**, 91 (1905).
- [40] L. Landau and E. Teller, On the theory of sound dispersion, *Phys. Z. Sowjetunion* **10**, 34 (1936); *Collected Papers of L. D. Landau*, edited by D. Ter Haar (Pergamon, Oxford, 1965), pp. 147–153.
- [41] G. Benettin, L. Galgani, and A. Giorgilli, Realization of holonomic constraints and freezing of high-frequency degrees of freedom in the light of classical perturbation-theory. Part II, *Commun. Math. Phys.* **121**, 557 (1989).
- [42] O. Baldan and G. Benettin, Classical “freezing” of fast rotations. A numerical test of the Boltzmann-Jeans conjecture, *J. Stat. Phys.* **62**, 201 (1991).